

Energy transfers in surface wave-averaged equations

Lars Czeschel^a Carsten Eden^a

^a *University of Hamburg*

arXiv:2311.13354v1 [physics.ao-ph] 22 Nov 2023

Corresponding author: Lars Czeschel, lczeschel@uni-hamburg.de

ABSTRACT: Ocean surface gravity waves play an important role for the air-sea momentum fluxes and the upper ocean mixing, and knowledge of the sea state leads in general circulation models to improved estimates of the ocean energy budget and allows to incorporate surface wave impacts, such as Langmuir turbulence. However, including the Stokes drift \mathbf{u}^S , in phase-averaged equations for the Eulerian mean motion leads to an Eulerian energy budget which is physically difficult to interpret. In this note, we show that a Lagrangian energy budget allows for a closed energy budget, in which all terms connecting the different energy compartments correspond to well known energy transfer terms. We show that the so-called Coriolis-Stokes force does not lead to an energy transfer between surface gravity waves and oceanic mean motions as previously suggested. Instead, the Coriolis-Stokes force transfers energy between the Eulerian mean kinetic energy, $MKE_E = \frac{1}{2}\bar{\mathbf{u}} \cdot \bar{\mathbf{u}}$, and a mean energy compartment which is the product of the mean Eulerian velocity $\bar{\mathbf{u}}$ and the mean Stokes drift $\bar{\mathbf{u}}^S$, $MKE_{ES} = \bar{\mathbf{u}} \cdot \bar{\mathbf{u}}^S$. Both energy forms are a result of the unnatural split-up of the Lagrangian velocity into Eulerian velocity and the Stokes drift. In an energy budget for the Lagrangian mean kinetic energy, the work done by the Coriolis-Stokes force does not contribute, and should be used to estimate the kinetic energy balance in the wave-affected surface mixed layer. The Lagrangian energy budget is used to discuss an energetically consistent framework which can be used to couple a general circulation ocean model to a surface wave model.

1. Introduction

In a non-rotating frame, Stokes (1847) established that surface gravity waves induce a mean flow in the direction of wave propagation, known as the Stokes drift \mathbf{u}^S . Craik and Leibovich (1976) were able to incorporate \mathbf{u}^S in wave averaged Boussinesq momentum equations for the Eulerian velocity \mathbf{u} . Including the Coriolis force, the equations are given by (e.g. Huang (1979), Leibovich (1980)):

$$\partial_t \mathbf{u} + (\mathbf{u} \cdot \nabla) \mathbf{u} = -\mathbf{f} \times \mathbf{u} - \underbrace{\mathbf{f} \times \mathbf{u}^S}_{F_{CS}} + b\mathbf{z} - \nabla p^* + \underbrace{\mathbf{u}^S \times \boldsymbol{\omega}}_{F_V} + \mathbf{D}_u \quad (1)$$

Here, $b = -g\rho/\rho_0$ denotes buoyancy, $\boldsymbol{\omega} = \nabla \times \mathbf{u}$ is the Eulerian vorticity, \mathbf{f} is the Coriolis parameter, and \mathbf{D}_u indicates dissipation of Eulerian momentum. Surface wave impacts enter the equation through \mathbf{u}^S and are given by the Coriolis-Stokes force F_{CS} , the vortex force F_V , and the modified pressure $p^* = p/\rho_0 + \frac{1}{2}[(\mathbf{u} - \mathbf{u}^S)^2 - \mathbf{u}^2]$. The equations are usually referred to as 'Craik-Leibovich equations' and are widely used to study the impact of surface waves on the oceanic surface mixed layer and Ekman-spiral solution (e.g. Skillingstad and Denbo (1995), McWilliams et al. (1997), Polton et al. (2005)).

The Coriolis Stokes force F_{CS} originates from the wave-induced Reynolds stresses, and leads in an inviscid ocean to an Eulerian flow which is exactly opposite to the Stokes drift, resulting in a vanishing Lagrangian mean flow (Hasselmann 1970). This result is in agreement with previous findings, that in a rotating ocean, a Lagrangian mass transport cannot arise from a steady wave field (Ursell and Deacon (1950), Pollard (1970)). Hasselmann (1970) further established that the Coriolis Stokes force leads to surface wave driven inertial oscillations. The vortex force F_V causes vorticity to tilt in the direction of the Stokes drift. The result are coherent vortices known as Langmuir circulation (Craik and Leibovich 1976). The associated Langmuir turbulence is often a dominant source for turbulent motions and mixing in the oceanic mixed layer (Belcher et al. 2012). Note, that the term 'Langmuir turbulence' sometimes include the shear driven turbulence of the Eulerian return flow, called anti-Stokes flow.

Global and regional climate models do not resolve Langmuir turbulence, however numerous parameterizations exist and have been tested in such models (e.g. Fan and Griffies (2014), Ali et al. (2019)). The parameterizations usually rely on the knowledge of the Stokes drift. Under the assumption of a fully developed sea, the Stokes drift can be approximated by using the local wind.

However, such a sea state in equilibrium seems to be a rather poor assumption (Hanley et al. 2010). Another possibility is to use a third generation surface wave model like WAM (Komen et al. 1996) or WAVEWATCH III (2016). Several studies have coupled such a surface wave model to regional or global climate models by using some form of the Craik-Leibovich equation (e.g. Breivik et al. (2015), Li et al. (2016), Sun et al. (2022)) or phase-averaged equations of even higher order in vertical shear (Couvelard et al. (2020)).

The Stokes drift obtained from surface wave models has also been utilized to estimate the energy input into the ocean. If the Craik-Leibovich equation (Eq. (1)) is used to form an energy equation for the Eulerian mean kinetic energy, $MKE_E = \frac{1}{2} \bar{\mathbf{u}} \cdot \bar{\mathbf{u}}$, a transfer term appears of the form $\partial_t MKE_E = -\bar{\mathbf{u}} \cdot (\mathbf{f} \times \bar{\mathbf{u}}^S)$. The overbar denotes an adequate averaging. The Coriolis force, despite being a fictitious force, contributes then in this energy equation to the energy budget which is difficult to understand. The above transfer term is considered to be an energy transfer from the surface waves to the Eulerian kinetic energy (e.g. Suzuki and Fox-Kemper (2016), hereafter SFK16) and has been used to calculate the energy input into the mixed layer (Liu et al. (2009), Sayol et al. (2016), Zhang et al. (2019), among others). On the global scale Liu et al. (2009) estimated an energy input of 0.29 Tw in the Ekman layer through the work done by the Coriolis-Stokes force, which is a significant share of other important transfer rates in the global ocean energy cycle. However, at least to our knowledge, no energy equation for surface waves was derived which shows the corresponding transfer term of opposite sign. Broström et al. (2014) and Weber et al. (2015) discussed some inconsistencies in the energy budget related to the Coriolis-Stokes force. They both conclude that the Coriolis-Stokes force plays no role in the energy budget, if the budget is integrated vertically to the moving material surface, i.e. in a Lagrangian framework.

If Eq. (1) is used to form an energy equation for the Eulerian turbulent kinetic energy, $TKE_E = \frac{1}{2} \overline{\mathbf{u}' \cdot \mathbf{u}'}$, a transfer term appears of the form $\partial_t TKE_E = -\overline{\mathbf{u}' w'} \cdot \partial_z \bar{\mathbf{u}}^S$ (McWilliams et al. 1997). It is interpreted as a transfer from surface wave energy into TKE_E and originates from the Stokes term in the modified pressure p^* . The transfer term was also derived from rapid distortion theory (Teixeira and Belcher 2002) and from generalised Lagrangian mean theory (Ardhuin and Jenkins 2006). Apart from breaking waves, this transfer often dominates the TKE budget in the ocean mixed layer (Belcher et al. 2012) and is associated with Langmuir circulation, and thus may also

play an important role in the ocean energy cycle. It is the aim of this study to integrate all such energy transfers into a meaningful and consistent Lagrangian framework.

In Section 2 we discuss the mean kinetic energy equations in this Lagrangian framework which allow for a closed energy budget with well known energy transfer terms. Large eddy simulations are used to visualise some important energy transfers in idealised experiments in Section 3. As the model community starts to become aware of energy consistency (e.g. Eden et al. (2014)), we discuss in Section 4, how such a consistent framework could be realised in a general circulation ocean model coupled to a surface wave model.

2. Energy budgets

a. Mean kinetic energy

The surface-wave averaged Boussinesq momentum Eq. (1) can be rewritten in a mathematical identical form (SFK16):

$$\partial_t \mathbf{u} + (\mathbf{u}^L \cdot \nabla) \mathbf{u} + \mathbf{f} \times \mathbf{u}^L = b\mathbf{z} - \nabla p - u_i^L \nabla u_i^S + \mathbf{D}_u \quad (2)$$

Here, \mathbf{u} is the wave-averaged Eulerian velocity, $\mathbf{u}^L = \mathbf{u} + \mathbf{u}^S$ the Lagrangian velocity, i.e. the sum of the Eulerian velocity \mathbf{u} plus the Stokes drift \mathbf{u}^S with components u_i^L and u_i^S . Surface wave effects enter the momentum equations via the Stokes drift and modify the advection and the Coriolis term, i.e. the Coriolis-Stokes force adds to the "traditional" Coriolis force. The third term on the r.h.s. is the Stokes shear force and is responsible for Langmuir turbulence. Note, that Einstein summation convention is used here. For now we consider only molecular dissipation acting on the Lagrangian motion, so that $\mathbf{D}_u = \mu \nabla^2 \mathbf{u}^L$, with μ being the molecular viscosity.

A mean kinetic energy equation for the Eulerian velocity, $MKE_E = \frac{1}{2} \bar{u}_i \bar{u}_i$, can be derived by multiplying equation (2) by $\cdot \bar{\mathbf{u}}$, followed by a suitable averaging denoted by an overbar. The averaging should satisfy $\overline{\nabla_\alpha A} = \nabla_\alpha \bar{A}$ for $\alpha = (t, x, y, z)$, $\overline{\bar{A}} = \bar{A}$, and $\overline{\bar{A} \bar{B}} = \bar{A} \bar{B}$ for any quantities A and B . Suitable methods are therefore ensemble and horizontal averages. Here we choose horizontal averaging, as we will later show model results in a horizontally periodic domain. The velocity \mathbf{u} can be therefore split into $\mathbf{u} = \bar{\mathbf{u}} + \mathbf{u}'$, where the turbulent velocity \mathbf{u}' is the deviation from the mean velocity $\bar{\mathbf{u}}$. In the same way we split \mathbf{u}^L and \mathbf{u}^S . As all our velocities are

phase-averaged with respect to surface gravity waves, the above horizontal averaging relies on the non-trivial assumption that turbulent quantities are de-correlated from the wave phase. This might be especially problematic with respect to \mathbf{u}^S , however, we here follow SFK16 and keep this assumption for now.

$\partial_t MKE_E$ is then given by:

$$\begin{aligned}
\frac{\partial}{\partial t} MKE_E + \underbrace{\overline{u_j^L} \frac{\partial}{\partial x_j} MKE_E}_1 + \underbrace{\frac{\partial}{\partial x_j} (\overline{u_j p})}_2 + \underbrace{\frac{\partial}{\partial x_j} (\overline{u_i u_i' u_j^{L'}})}_3 - \underbrace{\frac{\partial}{\partial x_j} \left(\mu \overline{u_i} \frac{\partial \overline{u_i^L}}{\partial x_j} \right)}_4 = \\
\underbrace{\overline{u_i' u_j^{L'}} \frac{\partial \overline{u_i}}{\partial x_j}}_5 + \underbrace{\delta_{i,3} \overline{b u_i}}_6 - \underbrace{\mu \frac{\partial \overline{u_i}}{\partial x_j} \frac{\partial \overline{u_i^L}}{\partial x_j}}_7 - \underbrace{\epsilon_{ijk} \overline{u_i} f_j \overline{u_k^S}}_8 - \underbrace{\overline{u_i} \overline{u_j^L} \frac{\partial \overline{u_j^S}}{\partial x_i}}_9 - \underbrace{\overline{u_i} \overline{u_j^{L'}} \frac{\partial \overline{u_j^{S'}}}{\partial x_i}}_{10}
\end{aligned} \tag{3}$$

Eq. (3) distinguishes transport terms on the l.h.s. from exchange terms on the r.h.s. The terms 1 to 4 are advection of MKE_E , work done by pressure, transport by the Reynolds stresses, and transport by viscous stresses, respectively. These terms redistribute mean kinetic energy. Note, that here MKE_E is advected by the Lagrangian mean velocity $\overline{\mathbf{u}^L}$ and that the Reynolds stresses combine the deviations from the Eulerian and Lagrangian mean, i.e. $\overline{u_i' u_j^{L'}}$. Term 5 gives the exchange with turbulent kinetic energy, followed by the exchange with mean potential energy (term 6). The molecular dissipation of MKE_E is given by term 7. The dissipation is not positive definite, which depends whether the dissipation acts on the Eulerian or the Lagrangian velocity. The decision has consequences of either having a non-positive definite dissipation in the Eulerian energy or helicity budget (Holm 1996). We assume that the molecular dissipation acts on the Lagrangian velocity, which leads to a positive definite dissipation in the Lagrangian energy budget introduced further below.

The term 8 in Eq. (3) is the work done by the Coriolis-Stokes force. Finally, we have the somewhat unfamiliar terms 9 and 10 which both originate from the Stokes shear force. Eq. (3) is first given in a form which is similar to SFK16, who already derived the terms 8 to 10. These terms are absent in an energy equation without the presence of surface waves and therefore represent energy exchanges with surface wave energy (SFK16). To our knowledge, the full MKE_E equation in the current form is here presented for the first time.

Eq. (3) can be reformulated in the more familiar form:

$$\begin{aligned}
\frac{\partial}{\partial t} MKE_E + \underbrace{\overline{u_j} \frac{\partial}{\partial x_j} MKE_L}_{T1^E} + \underbrace{\frac{\partial}{\partial x_j} (\overline{u_j p})}_{T2^E} + \underbrace{\frac{\partial}{\partial x_j} (\overline{u_i u_i^{L'} u_j^{L'}})}_{T3^E} - \underbrace{\frac{\partial}{\partial x_j} \left(\mu \overline{u_i} \frac{\partial u_i^L}{\partial x_j} \right)}_{T4^E} = \\
\underbrace{\overline{u_i^{L'} u_j^{L'}} \frac{\partial \overline{u_i}}{\partial x_j}}_{E1^E} + \underbrace{\delta_{i,3} \overline{b u_i}}_{E2^E} - \underbrace{\mu \frac{\partial \overline{u_i}}{\partial x_j} \frac{\partial u_i^L}{\partial x_j}}_{E3^E} - \underbrace{\epsilon_{ijk} \overline{u_i} f_j u_k^S}_{E^4}
\end{aligned} \tag{4}$$

The reformulation allows for an easier interpretation of the individual terms and is given here for the first time. The labelling of the terms in Eq. (4) distinguishes transport terms T from exchange terms E . The advection term $T1^E$ in Eq. (4) is now expressed as the advection of Lagrangian mean kinetic energy, $MKE_L = \frac{1}{2} \overline{\mathbf{u}^L} \cdot \overline{\mathbf{u}^L}$, advected by the eulerian velocity $\overline{\mathbf{u}}$. The Reynolds stresses in term $T3^E$ and $E1^E$ are now the deviations from Lagrangian mean velocities. The unfamiliar terms 9 and 10 of Eq. (3) are absorbed into the more familiar terms $T1^E$, $T3^E$ and $E1^E$ of Eq. (4), i.e. in the latter form they can be interpreted as either transport terms or in case of $E1^E$ as an exchange with turbulent kinetic energy.

Adding $\partial_t \mathbf{u}^S$ on both sides of Eq. (2) allows to write a tendency equation for the Lagrangian velocity (Holm 1996):

$$\partial_t \mathbf{u}^L + (\mathbf{u}^L \cdot \nabla) \mathbf{u}^L + \mathbf{f} \times \mathbf{u}^L = b\mathbf{z} - \nabla p - \mathbf{u}^L \times (\nabla \times \mathbf{u}^S) + \mathbf{D}_u + \partial_t \mathbf{u}^S \tag{5}$$

The momentum equation Eq. (5) will be the cornerstone, on which our Lagrangian energy budget and suggested model framework relies. In contrast to Eq. (2), velocities are fully written in terms of \mathbf{u}^L and \mathbf{u}^S , i.e. the Eulerian velocity is absent. The term $-\mathbf{u}^L \times (\nabla \times \mathbf{u}^S) = -u_i^L \nabla u_i^S + (\mathbf{u}^L \cdot \nabla) \mathbf{u}^S$ contains the Stokes shear term and the advection of \mathbf{u}^S . A temporal change in the Stokes drift $\partial_t \mathbf{u}^S$ can be interpreted as a forcing term for the Lagrangian velocity.

Multiplying Eq. (5) by $\cdot \overline{\mathbf{u}^L}$ and averaging leads then to a tendency equation for the Lagrangian mean kinetic energy $MKE_L = \frac{1}{2} \overline{u_i^L u_i^L}$:

$$\begin{aligned}
\frac{\partial}{\partial t} MKE_L + \underbrace{\overline{u_j^L} \frac{\partial}{\partial x_j} MKE_L}_{T1^L} + \underbrace{\frac{\partial}{\partial x_j} (\overline{u_j^L} \overline{p})}_{T2^L} + \underbrace{\frac{\partial}{\partial x_j} (\overline{u_i^L} \overline{u_i^{L'}} \overline{u_j^{L'}})}_{T3^L} - \underbrace{\frac{\partial}{\partial x_j} \left(\nu \frac{\partial}{\partial x_j} MKE_L \right)}_{T4^L} = \\
\underbrace{\overline{u_i^{L'}} \overline{u_j^{L'}} \frac{\partial \overline{u_i^L}}{\partial x_j}}_{E1^L} + \underbrace{\delta_{i,3} \overline{b} \overline{u_i^L}}_{E2^L} - \underbrace{\mu \frac{\partial \overline{u_i^L}}{\partial x_j} \frac{\partial \overline{u_i^L}}{\partial x_j}}_{E3^L} + \underbrace{\overline{u_i^L} \frac{\partial \overline{u_i^S}}{\partial t}}_{E7^L}
\end{aligned} \tag{6}$$

The labelling of Eq. (6) follows Eq. (4), i.e. the number indicates the physical interpretation of the term. A short version of Eq. (6), without the terms $T3^L$, $E1^L$ and $E2^L$, is also given in Holm (1996). We first notice that apart from the new forcing term $E7^L$, Eq. (6) represents the standard textbook form of a mean kinetic energy equation (e.g. Olbers et al. (2012), their Eq. 11.63), but here purely expressed using the Lagrangian velocity \mathbf{u}^L . The Coriolis force is absent in the energy budget for MKE_L . We further notice that the exchange term with turbulent Lagrangian energy, $E1^L$, includes $\overline{u_i^{L'}} \overline{u_j^{L'}} \partial_{x_j} \overline{u_i^S}$, which is missing in $E1^E$ of Eq. (4).

We propose energy equation Eq. (6) for MKE_L to be used for interpretation and quantification of energy transfers and budget in the surface wave effected ocean. Eq. (6) will be exploited in section 4, in order to establish an energetically consistent coupling between a surface wave and ocean model.

MKE_L can be split into different energy compartments:

$$MKE_L = \frac{1}{2} (\overline{\mathbf{u}} + \overline{\mathbf{u}^S}) \cdot (\overline{\mathbf{u}} + \overline{\mathbf{u}^S}) = MKE_E + MKE_S + MKE_{ES} \tag{7}$$

$MKE_S = \frac{1}{2} \overline{\mathbf{u}^S} \cdot \overline{\mathbf{u}^S}$ is the kinetic energy in the Stokes drift, its evolution is solely given by our prescribed forcing, i.e. $\partial_t MKE_S = \overline{\mathbf{u}^S} \cdot \partial_t \overline{\mathbf{u}^S}$. $MKE_{ES} = \overline{\mathbf{u}} \cdot \overline{\mathbf{u}^S}$ is some mixed Eulerian velocity/Stokes drift energy. By construction MKE_{ES} is not always positive. A possible negative energy already shows that the split of MKE_L into the different compartments is a purely mathematical construct which cannot be based on physical arguments. However, we follow this route for a moment here. A tendency equation for MKE_{ES} can be derived by multiplying Eq. (2) by $\cdot \mathbf{u}^S$

followed by averaging, and is given by

$$\begin{aligned}
\frac{\partial}{\partial t} MKE_{ES} + \underbrace{\overline{u_j^S} \frac{\partial}{\partial x_j} MKE_L}_{T1^{ES}} + \underbrace{\frac{\partial}{\partial x_j} (\overline{u_j^S \overline{p}})}_{T2^{ES}} + \underbrace{\frac{\partial}{\partial x_j} (\overline{u_i^S u_i^{L'} u_j^{L'}})}_{T3^{ES}} - \underbrace{\frac{\partial}{\partial x_j} \left(\mu \overline{u_i^S} \frac{\partial \overline{u_i^L}}{\partial x_j} \right)}_{T4^{ES}} = \\
\underbrace{\overline{u_i^{L'} u_j^{L'}} \frac{\partial \overline{u_i^S}}{\partial x_j}}_{E1^{ES}} + \underbrace{\delta_{i,3} \overline{b} u_i^S}_{E2^{ES}} - \underbrace{\mu \frac{\partial \overline{u_i^S}}{\partial x_j} \frac{\partial \overline{u_i^L}}{\partial x_j}}_{E3^{ES}} - \underbrace{\epsilon_{ijk} \overline{u_i^S} f_j \overline{u_k}}_{E4^{ES}} + \underbrace{\overline{u_i} \frac{\partial \overline{u_i^S}}{\partial t}}_{E7^{ES}}
\end{aligned} \tag{8}$$

By construction, the individual terms of Eq. (8) can be added to the terms of the tendency equations for MKE_E and MKE_S to give the tendency equation for MKE_L . The triple product of term $E4^{ES}$ in Eq. (8) corresponds to the triple product of term $E4^E$ in Eq. (4) only with opposite sign, i.e. the work done by the Coriolis-Stokes force exchange energy between MKE_{ES} and MKE_E . As both are part of the Lagrangian energy MKE_L , the work done by the Coriolis-Stokes force does not appear in the budget for MKE_L .

A physical interpretation and/or justification for MKE_{ES} is lacking, and so is any exchange between MKE_{ES} and MKE_E . We therefore encourage to use the the Lagrangian energy MKE_L budget, were such an energy transfer term based on the fictitious Coriolis force is absent.

b. Turbulent kinetic energy

An equation for the turbulent Lagrangian kinetic energy, $TKE_L = \frac{1}{2} \overline{\mathbf{u}^{L'} \cdot \mathbf{u}^{L'}}$ can be derived by multiplying Eq. (5) by $\cdot \mathbf{u}^{L'}$ and averaging:

$$\begin{aligned}
\frac{\partial}{\partial t} TKE_L + \underbrace{\overline{u_j^L} \frac{\partial}{\partial x_j} TKE_L}_{T1^{L'}} + \underbrace{\frac{\partial}{\partial x_j} \overline{u_j^{L'} p'}}_{T2^{L'}} + \underbrace{\frac{\partial}{\partial x_j} \left(\frac{1}{2} \overline{u_j^{L'} u_i^{L'} u_i^{L'}} \right)}_{T3^{L'}} - \underbrace{\frac{\partial}{\partial x_j} \left(\mu \frac{\partial}{\partial x_j} TKE_L \right)}_{T4^{L'}} = \\
\underbrace{-\overline{u_i^{L'} u_j^{L'}} \frac{\partial \overline{u_i^L}}{\partial x_j}}_{E1^{L'}} + \underbrace{\delta_{i,3} \overline{b'} u_i^{L'}}_{E2^{L'}} - \underbrace{\mu \frac{\partial \overline{u_i^{L'}}}{\partial x_j} \frac{\partial \overline{u_i^{L'}}}{\partial x_j}}_{E3^{L'}} + \underbrace{\overline{u_i^{L'}} \frac{\partial \overline{u_i^{S'}}}{\partial t}}_{E7^{L'}}
\end{aligned} \tag{9}$$

The tendency equation for TKE_L represents again the textbook form of a turbulent kinetic energy equation (e.g. Olbers et al. (2012), their Eq. 11.62), with the addition of a forcing term $E7^{L'}$. The transport terms $T1^{L'}$ to $T4^{L'}$ are Lagrangian advection of TKE_L , work done by pressure fluctuation,

transport by Reynolds-, and by viscous stresses, respectively. Term $E1^{L'}$ represents the exchange term with MKE_L and corresponds to term $E1^L$ of Eq. (6). Term $E2^{L'}$ gives the exchange with turbulent potential energy, and $E3^{L'}$ describes the molecular dissipation of TKE_L .

Similar to the mean kinetic energy, we can split TKE_L into different compartments, i.e. $TKE_L = TKE_E + TKE_S + TKE_{ES}$. $TKE_S = \frac{1}{2} \overline{\mathbf{u}^{S'} \cdot \mathbf{u}^{S'}}$ is the kinetic energy in the Stokes drift fluctuations, its evolution is given by the forcing term, i.e. $\partial_t TKE_S = \overline{\mathbf{u}^{S'} \cdot \partial_t \mathbf{u}^{S'}}$. $TKE_{ES} = \overline{\mathbf{u}' \cdot \mathbf{u}^{S'}}$ is a unfamiliar mixed turbulent Eulerian/Stokes energy which is not positive definite. Finally, $TKE_E = \frac{1}{2} \overline{\mathbf{u}' \cdot \mathbf{u}'}$ is the Eulerian turbulent kinetic energy, its evolution is given by:

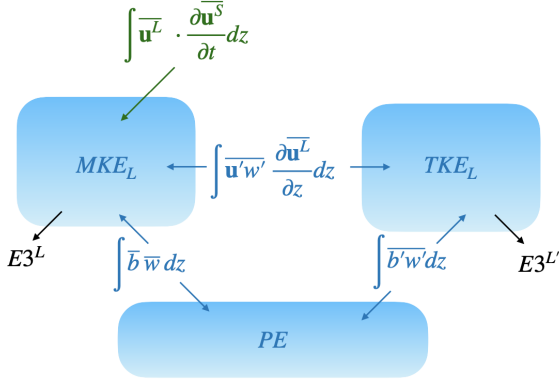
$$\begin{aligned} \frac{\partial}{\partial t} TKE_E + \underbrace{\overline{u_j} \frac{\partial}{\partial x_j} TKE_L}_{T1^{E'}} + \underbrace{\frac{\partial}{\partial x_j} \overline{u'_j p'}}_{T2^{E'}} + \underbrace{\frac{\partial}{\partial x_j} \left(\frac{1}{2} \overline{u'_j u_i^{L'} u_i^{L'}} \right)}_{T3^{E'}} - \underbrace{\frac{\partial}{\partial x_j} \left(\mu u'_i \frac{\partial u_i^{L'}}{\partial x_j} \right)}_{T4^{E'}} = \\ \underbrace{-\overline{u'_i u'_j} \frac{\partial \overline{u_i^L}}{\partial x_j}}_{E1^{E'}} + \underbrace{\delta_{i,3} \overline{b' u'_i}}_{E2^{E'}} - \underbrace{\mu \frac{\partial u'_i}{\partial x_j} \frac{\partial u_i^{L'}}{\partial x_j}}_{E3^{E'}} - \underbrace{\overline{\epsilon_{ijk} u'_i f_j u_k^{S'}}}_{E4^{E'}} \end{aligned} \quad (10)$$

The term $E4^{E'}$ represents work done by the fluctuating part of the Coriolis-Stokes force. It does not show up in the TKE_L budget, as it exchanges energy with TKE_{ES} in the same way as its mean part exchanges energy between MKE_E and MKE_{ES} . The shear production term $E1^{E'}$ includes the full Lagrangian shear, i.e. it represents only partly an exchange with MKE_E given by the Eulerian shear production, but additionally exchange energy with MKE_{ES} given by the Stokes shear production term $E1^{ES}$.

c. Lagrangian vs. Eulerian energy budget

In order to simplify the comparison between Lagrangian and Eulerian framework, we consider the plausible assumption that $\mathbf{u}^{S'} = 0$. The result is that TKE_L and TKE_E , and their corresponding tendency Eq. (9) and (10) are identical. Schematics of the vertically integrated energy budgets which then follow are given in Fig. (1). Our advocated Lagrangian framework has a closed mechanical energy budget. Compartments and the well known energy transfer terms are given in black in Fig. (1a). Exchange terms with other energy compartments are colored in blue. Exchanges

a) Lagrangian energy budget



b) Eulerian energy budget

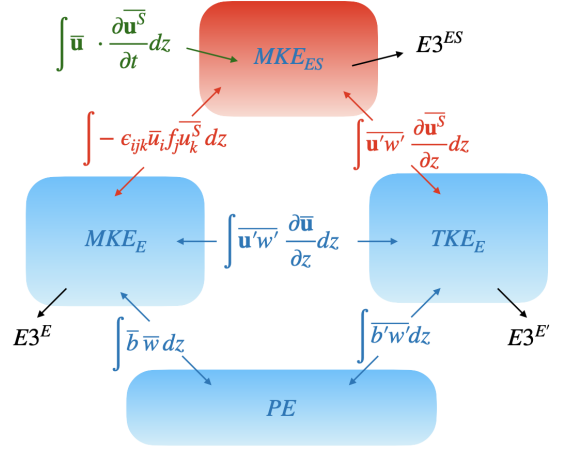


FIG. 1. Schematic of the energy exchanges between different compartments (boxes) for a) the Lagrangian and b) the Eulerian framework. Blue transfer terms give transfers within the mechanical energy budget of the ocean. Green transfer terms give exchanges with surface wave energy through temporal changes in the Stokes drift, and black transfer terms give exchanges with internal energy through molecular dissipation ($E3$ terms). Finally, red transfer terms give exchanges with the physically difficult to interpret compartment MKE_{ES} . Energy fluxes at the vertical boundaries and lateral flux divergences are not shown.

with internal energy through molecular dissipation are given by the terms $E3^L$ and $E3^{L'}$ of Eq. (6) and Eq. (9), respectively. The only term, which exchange energy with "external" surface wave energy in this framework, is given by the forcing term $\int \bar{\mathbf{u}}^L \cdot \partial_t \bar{\mathbf{u}}^S dz$. Note, that the term "external" surface wave energy is used here, as the inclusion of the Stokes drift in MKE_L represents already some form of phase-averaged kinetic wave energy. Typically the wind stress, Stokes drift and near surface Lagrangian velocity are roughly aligned in the same direction, so that one can expect an overall energy transfer from the waves to oceanic motions by the forcing term, but exceptions seem possible.

Previous studies have interpreted the Eulerian mechanical energy budget (Fig. (1b)). The red energy transfer terms were interpreted as an energy exchange with surface wave energy (e.g. SFK16). However, surface wave energy equations showing these terms are lacking. A notable exception is the Stokes shear production term in the wave energy equation of Teixeira and Belcher (2002). By splitting up MKE_L in the different compartments MKE_E , MKE_{ES} , and MKE_S , we

showed that the red transfer terms can be interpreted as an exchange of MKE_E and TKE_E with MKE_{ES} . The $MKE_{ES} = \bar{\mathbf{u}} \cdot \overline{\mathbf{u}^S}$ compartment is given in red in (Fig. (1b)) because of its dubious physical meaning, for example, it is not positive definite. As the definition of MKE_{ES} includes the Eulerian velocity, there seems no reason to consider MKE_{ES} as part of the surface wave energy. Any physical interpretation of MKE_{ES} or the associated energy exchanges is very difficult. We therefore recommend to use the Lagrangian energy budget for quantification and interpretation of the energy transfers. Using idealized numerical experiments, we will show in the next section, that a Lagrangian framework can lead to complete different results in the energy transfers and budgets compared to the Eulerian framework.

In contrast to the energy transfer associated with the Coriolis-Stokes force, we do not wish to challenge the well-established interpretation of the Stokes shear production term $\overline{u'_i u'_j} \partial_x \overline{u_i^S}$ as an exchange between turbulence and surface wave energy. In the Lagrangian energy framework this can be interpreted as follows: the Stokes shear production term removes surface wave energy, which causes a change in the Stokes drift. The same amount of energy transfer is thus also contained in $\mathbf{u}^L \cdot \partial_t \mathbf{u}^S$. Note, however, that changes in the surface wave energy due to wave growth and breaking are considered to be much larger than due to the Stokes shear production term (Ardhuin et al. 2010).

The energy transfers through wave breaking and surface wave stresses can be interpreted as vertical boundary conditions for the transport terms labelled T3 and are not contained in the schematic in Fig. (1). Implications for a large-scale numerical model framework will be discussed in Section 4.

3. Numerical model experiments

Although the results in this study are essentially analytically, we visualise some of our findings using a numerical model. The model is designed to do large eddy simulations and is fully three dimensional with lateral cyclic boundary conditions. At the vertical boundaries, we use no-flux boundary conditions. A sponge layer damps velocities near the bottom, in order to prevent reflection of internal waves. The model integrates the surface-wave averaged Boussinesq momentum given

by Eq. (2) and a buoyancy equation of the form:

$$\partial_t b + (\mathbf{u}^L \cdot \nabla) b = D_b \quad (11)$$

The sub-grid scale closure follows Ducros et al. (1996), with a turbulent eddy viscosity μ_t operating on the Eulerian velocity, so that $\mathbf{D}_u = \nabla \mu_t \nabla (u^L - u^S)$. $D_b = \nabla \kappa_t \nabla b$, with a turbulent eddy diffusivity is $\kappa_t = \mu_t / Pr$, and a Prandtl number of $Pr = 0.7$.

The wave forcing is given by a prescribed Stokes drift which corresponds to monochromatic, uni-directional deep water wave:

$$u_{eq}^S = u_0^S \exp\left(\frac{z}{D_s}\right) \quad (12)$$

$D_s = (2k)^{-1}$ denotes the depth penetration scale, k the wave number, and $u_0^S = a^2 \omega k$ the surface Stokes drift, a as the amplitude, g the gravitational acceleration, and $\omega = \sqrt{gk}$ the frequency. We choose typical swell conditions with a wave length of $\lambda = 100m$, an amplitude of $a = 1.5m$, and a surface Stokes drift in positive x-direction of $u_0^S = 0.11 \frac{m}{s}$, leading to a depth penetration scale of $\sim 8m$. For the growth of swell, we follow the analytical solution of Wagner et al. (2021):

$$u^S(z, t) = u_{eq}^S(z) \left[1 - \exp\left(\frac{-t^2}{2T_w^2}\right) \right] \quad (13)$$

Here, $u_{eq}^S(z)$ is the equilibrated Stokes drift as given by Eq. (12), and T_w is a growth time scale, we chose $T_w = 2h$. The model uses a rigid-lid and we do not consider a wavy surface. A discussion of the Eulerian Stokes drift, which lies between the crests and troughs, is given by Broström et al. (2014).

a. Laminar flow

The focus of the first experiment is on mean kinetic energies. The model is initialised with a constant stratification of $N^2 = 5.0 \times 10^{-4} s^{-2}$. Although the Stokes shear term is included, the setup is chosen in a way, that the model does not generate Langmuir turbulence, i.e. shear and Langmuir instabilities are not able to overcome the initial stratification. This also keeps the turbulent viscosity and diffusivity at the lower limit, which corresponds to molecular friction and diffusion. The results are basically one dimensional in the vertical, and all velocities can be considered as mean quantities.

The lateral cyclic boundary conditions leads to a vanishing mean vertical velocity. The Coriolis frequency of $\mathbf{f} = f\mathbf{z} = 7.29 \times 10^{-5} s^{-1}$ corresponds to an inertial period of one day.

In order to see how surface waves drive inertial oscillations theoretically, we make the following assumptions. We consider a linear, inviscid ocean away from lateral boundaries, so that no horizontal pressure gradient can be established on the considered scales. If we choose a horizontal Stokes drift of the form $u^S(z, t)$ the horizontal components of Eq. (5) simplify to

$$\partial_t u^L - f v = \partial_t u^S \quad (14)$$

$$\partial_t v^L + f u + f u^S = 0 \quad (15)$$

A time dependent Stokes drift will lead to inertial oscillations as shown by Hasselmann (1970). In steady state, the mass transport due to surface waves is exactly zero as the Stokes drift is balanced by the Eulerian anti-Stokes flow, i.e. $u^L, v^L = 0$ and $u^S = -u$.

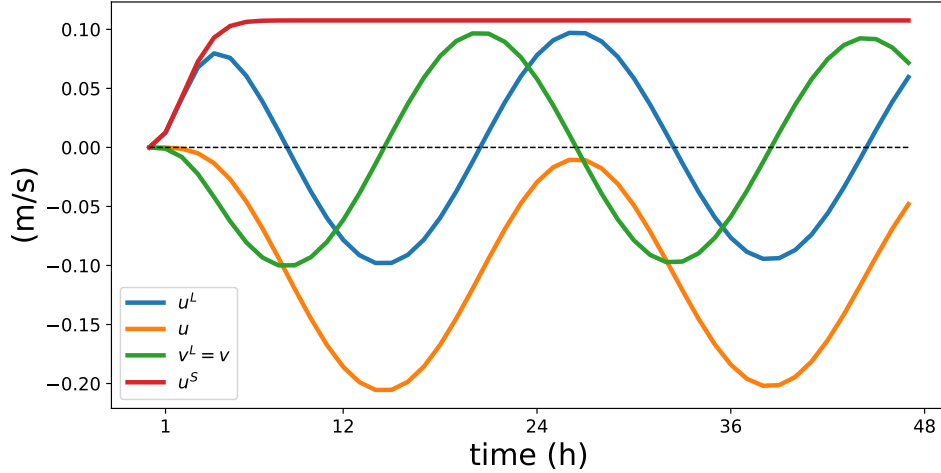


FIG. 2. Time evolution of surface velocities: Eulerian zonal velocity (orange), Lagrangian zonal velocity (blue), Eulerian/Lagrangian meridional velocity (green), and zonal Stokes drift (red)

Although the non-linear and inviscid assumptions are not made in our model experiment, the results corresponds to Eqs. (14) and (15). Figure (2) shows the different velocity compartments at the sea surface. The model is forced by the arrival of swell, i.e. $\partial_t u^S$ in the first few hours according to Eq. (13) with a maximum forcing at $T_W = 2h$. The forcing leads to nearly ideal inertial oscillations with vanishing time mean in the Lagrangian velocities. As the Stokes drift is only in

zonal direction, the meridional component of the Eulerian and Lagrangian velocities are identical. The amplitude of the inertial oscillations reaches close to the magnitude of the Stokes drift and depends on the ratio between T_w and the inertial period. If T_w goes to zero, the amplitudes of the Stokes drift and inertial oscillations will be equal. The Eulerian velocity is therefore always negative for a positive Stokes drift. If we average over one inertial period, the Eulerian velocity will oppose the Stokes drift $u = -u^S$, known as the anti-Stokes flow. The model therefore reproduces the findings of Hasselmann (1970), and averaged over an inertial oscillation, the no net mass flux of Ursell and Deacon (1950).

In our simplified setting the Eulerian and Lagrangian mean kinetic energy Eqs. (4) and (6) reduce to:

$$\partial_t MKE_E = -\bar{\mathbf{u}} \cdot f\mathbf{z} \times \bar{\mathbf{u}}^S \quad (16)$$

$$\partial_t MKE_L = \bar{\mathbf{u}}^L \cdot \partial_t \bar{\mathbf{u}}^S \quad (17)$$

Changes in MKE_E are induced by the work done by the Coriolis-Stokes force. As noticed by Polton (2009), the term $\mathbf{u} \cdot f\mathbf{z} \times \mathbf{u}^S$ is a scalar product between a phase-averaged velocity and a phase-averaged non-linear momentum term (wave Reynolds stress), where the latter only gives $f\mathbf{z} \times \mathbf{u}^S$ after phase-averaging. Therefore, the energy equation should be derived before phase-averaging, as wave correlated terms could give rise to an additional term in the energy budget. We checked that for our monochromatic wave, to find out that these contribution can be safely neglected here. In the tendency equation for the MKE_L no Coriolis-Stokes force appears and the evolution is dependent on the forcing, i.e. $\bar{\mathbf{u}}^L \cdot \partial_t \bar{\mathbf{u}}^S$. As outlined in the previous section $MKE_L = MKE_E + MKE_{ES} + MKE_S$. The two remaining compartments are given by

$$\partial_t MKE_{ES} = \bar{\mathbf{u}} \cdot f\mathbf{z} \times \bar{\mathbf{u}}^S + \bar{\mathbf{u}} \cdot \frac{\partial \bar{\mathbf{u}}^S}{\partial t} \quad (18)$$

$$\partial_t MKE_S = \bar{\mathbf{u}}^S \cdot \frac{\partial \bar{\mathbf{u}}^S}{\partial t} \quad (19)$$

The vertically integrated energy budgets for the compartments are shown in Fig. (3) . The budget for MKE_E shows strong undulations during an inertial cycle. Averaged over an inertial period the budget is $0.46 \text{ m}^3 \text{ s}^{-2}$ and much higher than for the Lagrangian energy MKE_L , which

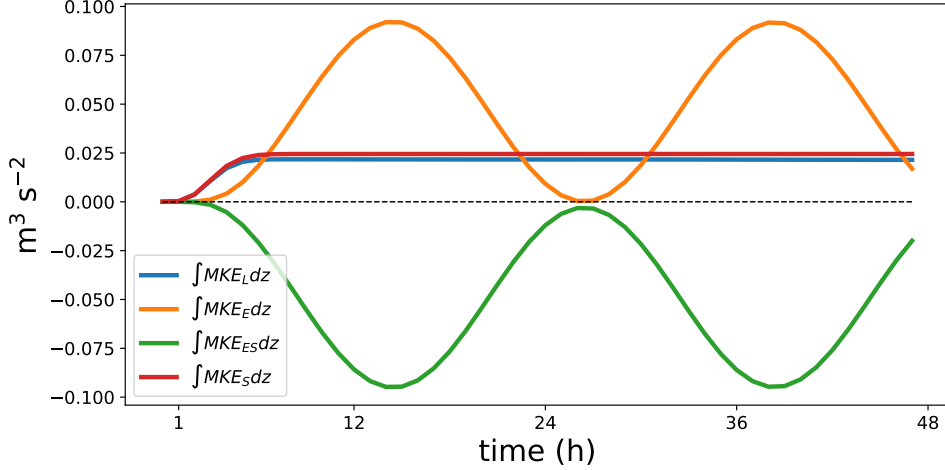


FIG. 3. Time evolution of vertically integrated mean kinetic energy compartments: Eulerian mean kinetic energy MKE_E (orange), Lagrangian mean kinetic energy MKE_L (blue), the mixed kinetic energy MKE_{ES} (green), and kinetic energy of the Stokes drift MKE_S (red). See text for details and definitions.

is $0.22 \text{ m}^3 \text{ s}^{-2}$. The exchange between MKE_E and MKE_{ES} through the Coriolis-Stokes term is the dominant signal. The sum of the MKE_E and the MKE_{ES} budget is still slightly negative as it is determined by the negative contribution of the r.h.s. of Eq. (18). As no further energy exchange terms are given, the difference in the budget between MKE_E and MKE_{ES} is identical to the difference between the two other compartments MKE_L and MKE_S . MKE_L gives the energy budget of the inertial oscillations (see also Fig. (2)) in this experiment, which in a more complex setting will decrease over time mainly through form stress at the base of the mixed layer and dissipation (see Czeschel and Eden (2019) and references therein). If all energy in the inertial oscillations is dissipated, MKE_L would be zero and any movement of fluid particles would stop. However, MKE_E would be still positive in such a steady state, as the Eulerian velocity would exactly oppose the Stokes drift. The physical interpretation of such an MKE_E budget is difficult, as the energy cannot be transferred to, for example, TKE .

Multiplying the integrated mean energies by reference density, e.g. $\rho_0 = 1000 \text{ kg/m}^3$, allows a comparison with the total kinetic energy of the surface waves of $E_{kin} = \frac{1}{4}g\rho_0 a^2 = 5518 \text{ J/m}^2$, with $a = 1.5 \text{ m}$ being the amplitude of our prescribed swell. After the initial forcing period, $\int \rho_0 MKE_S dz \approx \int \rho_0 MKE_L dz \approx 25 \text{ J/m}^2$, i.e. it is just a small fraction of the total kinetic energy of the surface waves. E_{kin} accounts for the full orbital motion, whereas MKE_S accounts

only for the Stokes drift, i.e. the deviation from a closed orbital loop. The MKE_L budget of $\approx 25 J/m^2$ corresponds to the energy loss of E_{kin} to inertial oscillation within the first ≈ 4 hours as given by the r.h.s of Eq. (17). In contrast to the Eulerian energy budget, the Lagrangian energy budget therefore allows for a clear physical interpretation of the exchange terms.

b. Turbulent flow

The impact of turbulence on surface waves and the associated Stokes drift is largely unknown. Applying the same eddy viscosity on the Stokes drift as used in mixing parameterizations for the upper ocean Eulerian currents seems not appropriate, as the energy loss would be much too strong (Ardhuin and Jenkins 2006). A physical explanation for the different impact of turbulence on the Stokes drift and the Eulerian current might be given by the overlapping time and spatial scales in wave dynamics and turbulence. For example, the time scale associated with Langmuir turbulence is often larger than the wave periods of typical wind waves, i.e. Langmuir turbulence might have no impact on such waves. The consequence for the energy budget would be that the exchange terms between MKE_L and TKE_L in Eqs. (6) and (9), i.e. $\overline{u_i^{L'} u_j^{L'} \frac{\partial u_i^L}{\partial x_j}}$, do not share the same Reynolds stresses as they act on the Eulerian or the Stokes drift shear. The Lagrangian shear production term should be then reformulated as $\overline{u_i^{L'} u_j^{L'} \frac{\partial u_i^E}{\partial x_j}} + \overline{u_i^{L'} u_j^{L'} \frac{\partial u_i^S}{\partial x_j}}$ with $\overline{u_i^{L'} u_j^{L'} \frac{\partial u_i^E}{\partial x_j}} \neq \overline{u_i^{L'} u_j^{L'} \frac{\partial u_i^S}{\partial x_j}}$, here the different overbars denote different averaging scales. Parameterizing these Reynolds stresses would then demand different scale-dependent eddy viscosities.

However, the different Reynolds stresses are difficult to realise in models using phase-averaged equations, like the Craik-Leibovich equations. Such models typically prescribe the Stokes drift, and possible impacts of turbulence on the Stokes drift are neglected. This is achieved by an eddy viscosity that acts only on the Eulerian velocity and by neglecting the advection of Stokes drift.

We follow this approach here, and repeat the experiment from the laminar case but with a uniform mixed layer of 50m ($N^2 = 0 s^{-2}$) on top of the stratified interior ($N^2 = 5.0 \times 10^{-4} s^{-2}$). We additionally cool the ocean for 6 hours with $10 Wm^{-2}$, in order to generate some initial turbulence. The surface wave forcing follows again Eq. (13) starting at $t=0$ after the cooling period, i.e. the model starts without mean kinetic energy, but has a vertically integrated turbulent kinetic energy of $TKE_L = 1.73 \times 10^{-4} m^3 s^{-2}$. TKE_L equals TKE_E in our set-up, as the Stokes drift is horizontally constant and $\mathbf{u}^{S'} = 0$. The large time and spatial scales of our swell forcing suggest that all generated

turbulence act on the Stokes drift shear. As we apply lateral cyclic boundary conditions, all vertical mean velocities are zero, and the evolution of the mean horizontal velocities are governed by

$$\partial_t \overline{u^L} - f \overline{v} = \partial_z \left(\overline{\mu_t \frac{\partial u}{\partial z}} - \overline{u'w'} \right) + \partial_t \overline{u^S} \quad (20)$$

$$\partial_t \overline{v^L} + f \overline{u} + f \overline{u^S} = \partial_z \left(\overline{\mu_t \frac{\partial v}{\partial z}} - \overline{v'w'} \right) \quad (21)$$

here μ_t is the turbulent eddy viscosity acting on the Eulerian velocity. Note again, that $v^S = 0$ in our experiment, which also gives $v^L = v$. In steady state, and assuming no-flux boundary conditions at the surface and somewhere in the stratified interior, only the vertical integrals of the Stokes drift and the anti-Stokes flow balances, so that $\int \overline{u^S} dz = -\int \overline{u} dz$ and $\int \overline{v} dz = 0$. This should be compared to the laminar case (Eq. 14 and 15), where the steady state solution was $\overline{u^S} = -u$. Resolved and unresolved turbulence are therefore shaping the vertical profiles of the Eulerian velocities. The assumption that turbulence acts solely on the Eulerian velocities has therefore strong consequences on the vertical gradients of $\overline{u^L}$, \overline{u} , and $\overline{u^S}$, and therefore also for the exchange between MKE_L and TKE_L as given by the Lagrangian shear production term.

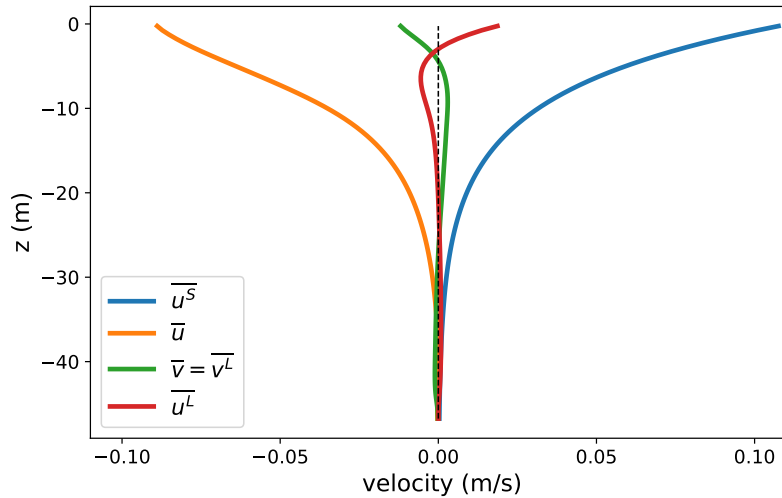


FIG. 4. Vertical profiles of horizontal averaged velocities. The velocities are averaged over one inertial period, or from model hour 12 to 36.

In our simulation, the vertical shear in the Stokes drift increases within the first ~ 6 h due to the growing swell. The result is a burst of turbulence driven by the developing Langmuir circulation.

The TKE budget is very similar to the findings of Wagner et al. (2021) and is not repeated here. Although the turbulence is not in equilibrium in such a setup, the "quasi steady-state" velocity profiles from our turbulent experiment are given in Fig. 4. The shaping of the anti-Stokes flow \bar{u} through turbulence is clearly visible. As predicted from Eq. (20) and Eq. (21) the vertical integrals of \bar{u} and \bar{u}^S cancel each other, and \bar{u}^L and \bar{v} integrate to zero. The differences between the profiles of \bar{u}^S and $(-\bar{u})$ depend on the amount of turbulence, which is rather weak in our experiment only driven by swell. For example, Langmuir turbulence driven by wind waves is usually stronger, and so are the differences between \bar{u} and \bar{u}^S . The differences become even larger, if other sources of turbulence also contribute.

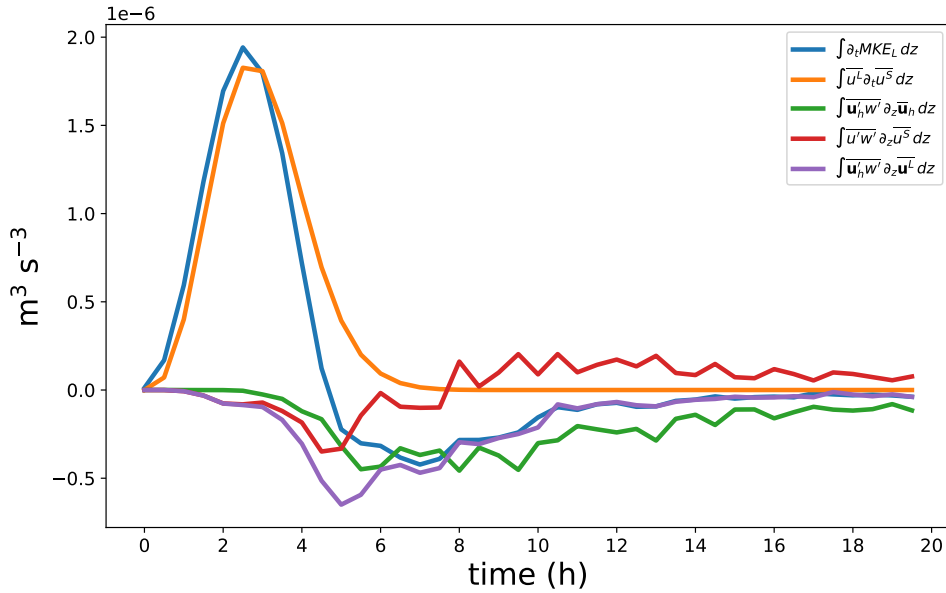


FIG. 5. Time evolution of vertically integrated mean kinetic energy tendency terms in m^3/s^3 . Shown are temporal changes in MKE_L (blue), the forcing due to a change in the Stokes drift (orange), the Lagrangian shear production term (purple), which consists of the Eulerian production term (shown in green) and the Stokes production term (red), and the The vector $\mathbf{u}_h = (u, v)$ denotes the horizontal components.

A detailed discussion of Langmuir turbulence driven by swell can be found in McWilliams et al. (2014) and Wagner et al. (2021) and is not the scope of the present study. We here concentrate on the impact on MKE_L . The evolution in the vertically integrated tendency terms of MKE_L are given in Fig. 5. Similar to the laminar case, the temporal change in MKE_L (blue) is initially given by the forcing term due to temporal changes in the Stokes drift (orange). As in the laminar case, the term

forces surface wave driven inertial oscillations. Around model hour three, Langmuir turbulence start to transfer energy from MKE_L to TKE_L as given by the Lagrangian shear production term (purple). After model hour 7 the change in MKE_L is solely given by Lagrangian shear production term. The Lagrangian shear production consists of the Eulerian (green) and Stokes shear production (red). The Stokes shear production term changes sign after ~ 9 hours. This is because the Reynolds stresses also changes sign, as they rotate with the Lagrangian mean flow, which is effected by the inertial oscillation (see McWilliams et al. (2014) for details). The Eulerian and Stokes shear production show some high frequent oscillations, which are largely compensated, so that the evolution of the Lagrangian shear production is much smoother. The compensation points to the somewhat artificial split-up of the Lagrangian shear production into Eulerian- and Stokes shear production in such models. The model is not able to differentiate between the different energy sources. Remember, that the Stokes shear production is interpreted as a direct energy exchange between surface wave energy and TKE (Teixeira and Belcher 2002).

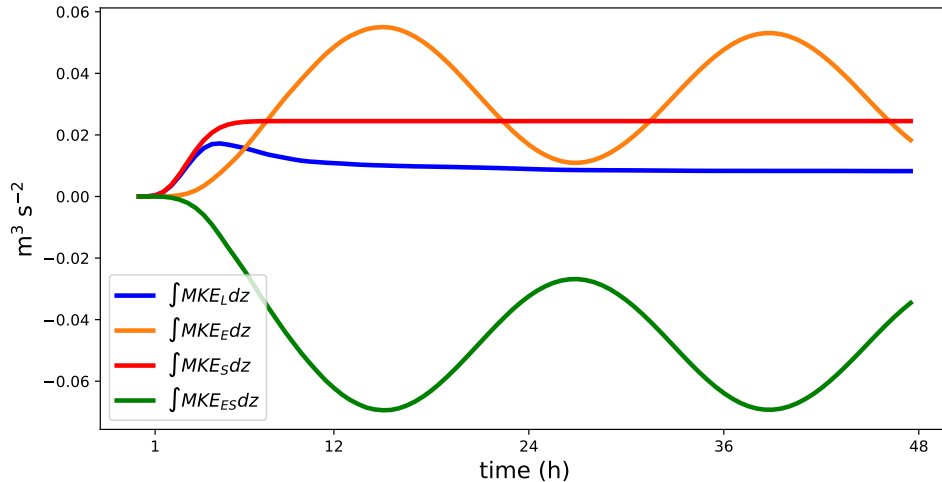


FIG. 6. Time evolution of vertically integrated mean kinetic energy compartments similar to figure 2 :Eulerian mean kinetic energy MKE_E (orange), Lagrangian mean kinetic energy MKE_L (blue), the mixed kinetic energy MKE_{ES} (green), and kinetic energy of the Stokes drift MKE_S (red). Note that MKE_S is solely based on the Stokes drift forcing which is identical to the laminar experiment.

Similar to the energy loss to inertial oscillations, the energy loss to TKE is only of minor importance for the energy budget of the surface waves on the here considered scales, but has strong

consequences for the oceanic motions. On longer time and spatial scales, however, such an energy loss might be an important contribution to swell dissipation (Ardhuin and Jenkins 2006).

The vertically integrated mean kinetic energy compartments are given in Fig. 6. In contrast to the laminar case (Fig. 3), MKE_L drops to a value much lower than the kinetic energy in the Stokes drift (MKE_S). The reduction in MKE_L is caused by the energy loss to TKE . MKE_E and MKE_{ES} again exchange energy through the work done by the Coriolis-Stokes force. This exchange dominates the evolution of the MKE_E budget. The loss to TKE through the Eulerian shear production, i.e. term E1 in Eq. (4), is not visible from this budget. MKE_E is again difficult to interpret, as it contains the largest energy budget, but most of this energy can not be exchanged with other physically meaningful energy compartments.

4. A framework for an energetically consistent coupling of a wave model to an ocean model

In this chapter we discuss several issues related to a large-scale general circulation ocean model coupled to a surface wave model. Special focus is given on consistent energy transfers. We concentrate on deep water waves and open ocean dynamics.

a. Model equations

In the suggested framework, the ocean model integrates the Lagrangian velocity $\mathbf{u}^L = \mathbf{u} + \mathbf{u}^S$. The Stokes drift \mathbf{u}^S , and its evolution, will be provided by the wave model. In the open ocean, the horizontal gradients in the Stokes drift, as given by wave models, are governed by the atmospheric synoptic scales (Haney et al. 2015), so that $\partial_x, \partial_y \mathbf{u}^L \gg \partial_x, \partial_y \mathbf{u}^S$. The divergence in the Stokes drift is therefore expected to be small, and allows us to assume $w^S = 0$, so that any horizontal divergence of the Stokes drift is compensated by w .

Exploiting the assumptions for the open ocean in momentum equation (5) and buoyancy equation (11), leads to the following equations to be used in large scale primitive equation ocean models:

$$\partial_t \mathbf{u}_h^L + (\mathbf{u}_h^L \cdot \nabla) \mathbf{u}^L + f \mathbf{z} \times \mathbf{u}^L = -\nabla_h p + \nabla \mu_t \nabla (\mathbf{u}^L - \mathbf{u}^S) + \partial_t \mathbf{u}_h^S \quad (22)$$

$$\partial_t b + (\mathbf{u}_h^L \cdot \nabla) b = \nabla \kappa_t \nabla b \quad (23)$$

Here, the subscript h denotes horizontal vector components, and μ_t and κ_t give turbulent viscosity and diffusivity, respectively. The Lagrangian velocity \mathbf{u}^L is the only prognostic velocity in the ocean model. Existing numerical codes for advection, the Coriolis force, dissipation, and the buoyancy equation can be used. The prognostic model velocity is then re-interpreted as the Lagrangian velocity u^L , similar to the re-interpretation of the model velocity as residual mean velocity including the Quasi-Stokes velocity in the transformed residual mean theory of McDougall and McIntosh (2001). Note, however, that dissipation should operate on $\mathbf{u} = \mathbf{u}^L - \mathbf{u}^S$.

Although it is well known that $\nabla \cdot \mathbf{u}^S \neq 0$ (McIntyre 1988), we ignore this divergence effect as it is usually quite small (Vanneste and Young 2022). The continuity equation is therefore given by $\nabla \cdot \mathbf{u}^L = 0$.

As a consequence of the open ocean assumption, the term $-\mathbf{u}^L \times (\nabla \times \mathbf{u}^S)$ in Eq. (5) can be neglected in the horizontal momentum equations (Eq. (22)). Using scaling arguments, SFK16 show the possible importance of the term for the vertical momentum equation. SFK16 suggest to modify the hydrostatic balance in primitive equation models to a "wavy hydrostatic balance" of the form, $\partial_z p - b = -u^L \partial_z u^S - v^L \partial_z v^S$. The necessity of including wave effects in the hydrostatic balance also depends on the resolved oceanic scales, and needs to be tested upon realization. Note, that using such a "wavy hydrostatic balance" would change the budget for MKE_L , and we recommend to use the "standard" hydrostatic balance, i.e. $\partial_z p = b$, for now.

b. Energy and momentum fluxes

A wave model typically integrates a version of the wave energy balance equation. For deep water waves in the open ocean, it reads

$$\partial_t F + \nabla \cdot (\mathbf{v}_g F) = S_{in} + S_{nl} + S_{diss} \quad (24)$$

where $F(\omega, \theta)$ is the two-dimensional wave energy spectrum, which gives the energy distribution over angular frequency ω and propagation direction θ . \mathbf{v}_g is the group velocity. The r.h.s. of Eq. (24) gives the local source terms, which consists of wind input S_{in} , non-linear transfer S_{nl} , and dissipation due to wave breaking S_{diss} .

The source terms can be utilised to determine the energy and momentum fluxes between wind, waves and ocean. The momentum flux $\boldsymbol{\tau}_{in}$ and energy flux Φ_{in} from wind to the waves are given

by (Janssen 2012):

$$\boldsymbol{\tau}_{in} = \rho_w g \int_0^{2\pi} \int_0^{\infty} \frac{\mathbf{k}}{\omega} S_{in} d\omega d\theta \quad (25)$$

$$\Phi_{in} = \rho_w g \int_0^{2\pi} \int_0^{\infty} S_{in} d\omega d\theta \quad (26)$$

and the fluxes from the waves to the ocean column by:

$$\boldsymbol{\tau}_{diss} = \rho_w g \int_0^{2\pi} \int_0^{\infty} \frac{\mathbf{k}}{\omega} S_{diss} d\omega d\theta \quad (27)$$

$$\Phi_{diss} = \rho_w g \int_0^{2\pi} \int_0^{\infty} S_{diss} d\omega d\theta \quad (28)$$

Here, ρ_w is the water density and $\mathbf{k} = (k_x, k_y)$ the wave number. Note, that the momentum fluxes are mostly determined through the high frequency part of the wave spectrum, as they scale with the inverse of the phase velocity $g = \omega/k$.

The atmospheric or air-side stress is given by $\boldsymbol{\tau}_a = \rho_a \mathbf{u}_*^2$, here ρ_a is the air density and \mathbf{u}_* the air friction velocity. The air-side stress is usually determined by a drag coefficient c_d and the wind speed in 10m height. As the drag coefficient c_d is dependent on the surface roughness, it should be modified by the sea state, and the wave model can be used to determine the surface roughness (see e.g. Breivik et al. (2015) for details).

The ocean side stress $\boldsymbol{\tau}_{oc}$ can be then considered as the atmospheric stress minus the residual momentum flux absorbed or released by the wave field

$$\boldsymbol{\tau}_{oc} = \boldsymbol{\tau}_a - \boldsymbol{\tau}_{in} - \boldsymbol{\tau}_{diss} \quad (29)$$

If wind increases over a calm ocean, the waves respond first by growing and $\boldsymbol{\tau}_{in} > -\boldsymbol{\tau}_{diss}$. As the waves mature, breaking intensifies, and so does the momentum transfer from the waves to the ocean $\boldsymbol{\tau}_{diss}$. At some point during wave growth, $\boldsymbol{\tau}_{diss}$ catch up with the momentum transfer from atmosphere to waves $\boldsymbol{\tau}_{in}$. The wave field then is in equilibrium and $\boldsymbol{\tau}_{in} = -\boldsymbol{\tau}_{diss}$ (Breivik et al. 2015). At this point the ocean side stress equals the air-side stress and Eq. (29) reduces to $\boldsymbol{\tau}_{oc} = \boldsymbol{\tau}_a$, which is the assumption made in classical bulk formulas, where $\boldsymbol{\tau}_{oc}$ is a function of the wind speed in 10m height. However, most of the time such an equilibrium is a poor assumption (Hanley et al.

2010). At some point the wind decreases, and the waves have a net momentum transfer into the ocean $\tau_{in} < -\tau_{diss}$.

The prognostic frequency range in wave models has an upper limit ω_c , above ω_c the wave spectrum is given by a widely accepted ω^{-5} power law. In the high-frequency diagnostic range, we assume that the wave field is always in equilibrium, so that $\tau_{oc} = \tau_a$ for $\omega > \omega_c$. The practical consequence is that Eq. (29) still holds, if we integrate τ_{in} and τ_{diss} over the prognostic range. A possible physical justification is provided by Chalikov and Belevich (1993), they argue that the small waves are sheltered by the large waves and by-pass wave growth, thereby directly driving mean motions. Such an interpretation is of course an over-simplification of the problem. How exactly momentum fluxes enter the ocean is subject of active research, but beyond the scope of the present study.

Similar to the momentum fluxes, the energy flux into the ocean is given by (Janssen 2012):

$$\Phi_{oc} = \Phi_{in} - \rho_w g \int_0^{2\pi} \int_0^{\omega_c} (S_{in} + S_{diss}) d\omega d\theta \quad (30)$$

which can be also written as

$$\Phi_{oc} = \rho_w g \int_0^{2\pi} \int_{\omega_c}^{\infty} S_{in} d\omega d\theta - \Phi_{diss} \quad (31)$$

i.e. the energy input consists of the direct energy gain from air in the diagnostic range and the dissipation of wave energy in the prognostic range, the latter is mainly the result of white capping. Note, the change in the limits of integration from Eq. (30) to Eq. (31).

Φ_{oc} is the energy transfer from the surface waves available to drive oceanic mean motions and turbulence. The kinetic energy of the ocean model in the resolved velocities is governed by the tendency Eq. (6) for MKE_L . To allow for a consistent energy transfers to sub-grid scales, we suggest using a second moment closure, for example a $k - \epsilon$ model. Such a closure integrates a TKE equation similar to Eq. (9) for TKE_L , however the transfer terms are parameterized. For simplicity we assume here a rigid-lid surface boundary condition, with $w^L = 0$ and $\tau_{oc} = \overline{\mathbf{u}^L w'}$ at $z = 0$. The energy gain of the ocean column is then governed by the transport terms T3 and the forcing terms E7 in Eqs. (6) and (9). Φ_{oc} should then match:

$$\Phi_{oc} = \overline{\mathbf{u}^L} \cdot \boldsymbol{\tau}_{oc} + \int \overline{\mathbf{u}^L} \cdot \partial_t \overline{\mathbf{u}^S} dz + \overline{\mathbf{u}^{L'}} \cdot \boldsymbol{\tau}'_{oc} + \int \overline{\mathbf{u}^{L'}} \cdot \partial_t \overline{\mathbf{u}^{S'}} dz + \epsilon_{break} \quad (32)$$

where ϵ_{break} denotes injection of *TKE* by breaking waves.

It is unclear, if either $\overline{\mathbf{u}^{L'}} \cdot \boldsymbol{\tau}'_{oc}$ or $\overline{\mathbf{u}^{L'}} \cdot \partial_t \overline{\mathbf{u}^{S'}}$ show any significant correlation in the primed terms, so that they could be possibly neglected. However, we combine them together with the also unknown dissipation due to breaking of waves, so that

$$\Gamma_{break} = \overline{\mathbf{u}^{L'}} \cdot \boldsymbol{\tau}'_{oc} + \int \overline{\mathbf{u}^{L'}} \cdot \partial_t \overline{\mathbf{u}^{S'}} dz + \epsilon_{break} \quad (33)$$

Γ_{break} can be determined in our coupled framework from Eq. (32), as the remaining terms can be obtained directly from the ocean or the surface wave model.

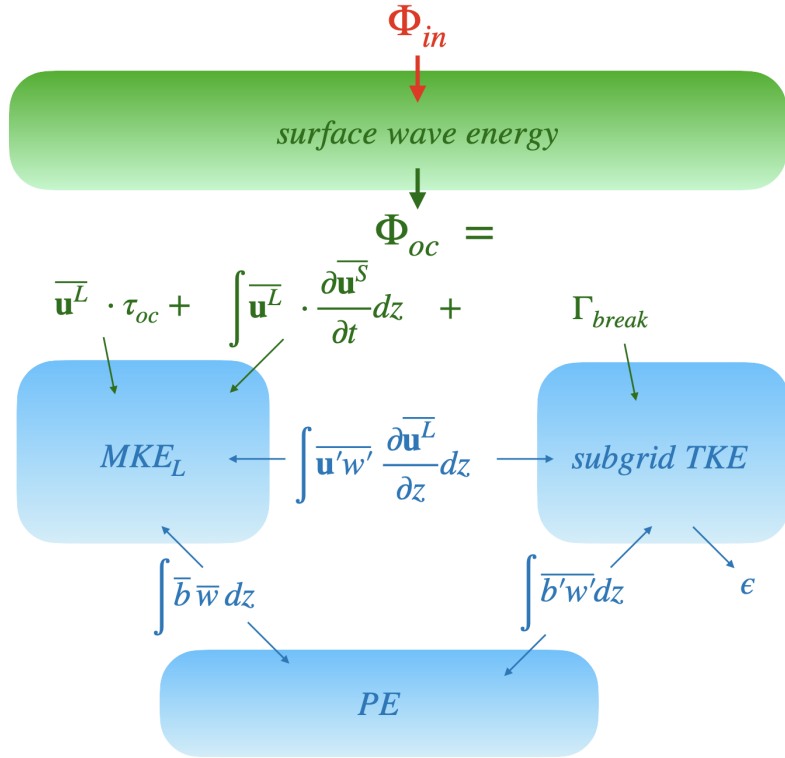


FIG. 7. Schematic of the energy exchanges between different compartments (coloured boxes). PE denotes potential energy and ϵ gives the integrated dissipation of subgrid *TKE*, i.e. the exchange with internal energy. Note, that the sign of the terms are associated with MKE_L if possible.

Figure (7) gives an overview of the different energy compartments and the involved energy transfers. The energy transfer from the wave model to the ocean is governed by Eq. (32). Γ_{break} goes directly into the subgrid TKE , whereas $\overline{\mathbf{u}^L} \cdot \overline{\boldsymbol{\tau}}_{oc}$ and $\int \overline{\mathbf{u}^L} \cdot \partial_t \overline{\mathbf{u}^S} dz$ drive MKE_L , i.e. resolved oceanic motion.

The Stokes production term $-\int \overline{\mathbf{u}^{L'} w'} \frac{\partial \overline{\mathbf{u}^S}}{\partial z} dz$ could be interpreted as a direct transfer from wave energy to subgrid TKE . In our framework it is part of the Lagrangian shear production term $\int \overline{\mathbf{u}^{L'} w'} \frac{\partial \overline{\mathbf{u}^L}}{\partial z} dz$, which transfers energy between MKE_L and subgrid TKE . To be fully energetically consistent, the shear production term should remove energy from the surface wave model and should be included in the wave dissipation term Φ_{diss} and therefore Φ_{oc} . Ardhuin et al. (2010) in their recent update on wave dissipation parameterization, discussed the inclusion of the shear production term. It was, however, neglected, as its contribution is considered to be very small.

c. Parameterizations

As mentioned above, we suggest to use a second moment closure for the subgrid TKE . Harcourt (2013) and Harcourt (2015) provide such a closure using the Craik-Leibovich equations, i.e. it involves a parameterization for the Stokes production term. The unknown Reynolds stresses are parameterized with two distinct eddy viscosities K_M and K_M^S , so that, e.g. $\overline{u'w'} = -K_M \partial_z u - K_M^S \partial_z u^S$. The eddy viscosities are derived from stability functions (see Harcourt (2013) for details). It should be however mentioned, that the distinct eddy viscosities lead to the same Reynolds stresses in the Eulerian and in the Stokes production term, i.e. it does not resolve possible issues with overlapping wave and turbulence scales, as discussed in the previous section.

Γ_{break} mainly consists of turbulence injected by breaking waves, the amount of energy is determined by eq. (32). The energy can be injected as a flux boundary condition in the equations for the second moment closure following Burchard (2001).

5. Summary and discussion

Based on the wave-averaged Craik-Leibovich equations including a prescribed Stokes drift, we present a closed Lagrangian energy framework. The only energy exchange of the Lagrangian ocean flow with surface waves is due to changes in the Stokes drift forcing. Advantages compared

to an Eulerian kinetic energy budget are that all energy transfer terms are well known and easy to interpret. In particular the work done by the "fictitious" Coriolis-Stokes force is absent in the Lagrangian energy budget. Previous studies have suggested that the work done by the Coriolis-Stokes force is associated with an energy transfer from the surface waves to the Eulerian kinetic energy. We argue that this energy gain is an artefact of the split-up of the Lagrangian kinetic energy into different compartments. The work done by the Coriolis-Stokes force is an exchange between the Eulerian kinetic energy and an energy compartment defined as $MKE_{ES} = \bar{\mathbf{u}} \cdot \overline{\mathbf{u}^S}$. The individual compartments of the Lagrangian kinetic energy are physically difficult to interpret, but the compensation between MKE_E and MKE_{ES} suggests that large parts of the Eulerian mean kinetic energy are not available for a transfer to turbulent kinetic energy and finally for mixing.

The ambiguity of the MKE_E budget suggests that previous estimates of the energy input into the ocean by wind and waves should be interpreted with care. Our Lagrangian framework suggests to ignore the work done by the Stokes-Coriolis force in such an estimate. The energy input into mean motions by the wind stress is $\mathbf{u}^L \cdot \boldsymbol{\tau}$ in our framework. At first glance this might be very different from previous estimates which used the Eulerian velocity or even the surface geostrophic velocity. However, a Stokes drift is usually accompanied by an Eulerian anti-Stokes flow of similar order (at least vertically integrated), reducing the impact of the Stokes drift.

The compensation of Stokes drift by an anti-Stokes flow is very dependent on the impact of turbulence on both. Unfortunately, such an impact on surface waves and the associated Stokes drift is largely unknown, hence ignored in most phase-averaged models. Nonetheless, the difference between Stokes drift shear and anti-Stokes flow shear plays an important role in the shear driven turbulence. The amount of compensation also modifies the surface Lagrangian velocity, and thus, the energy transfer from surface waves to mean motions.

In the current phase-averaged ocean models, the same Reynolds stresses act on the Eulerian and the Stokes shear. Overlapping temporal and spatial scales of turbulence and surface waves suggest that this assumption might not be very realistic. It might be valid for Swell though. At present, there is no solution in phase-averaged models, and how turbulence effect surface waves is a future task for the phase resolving modelling community.

Using our Lagrangian framework, we suggest an energetically consistent coupling between a surface wave model and a large-scale ocean model. We recommend to use the Lagrangian velocity

as prognostic velocity in the model as given by Eq. (22). Other forms of the Craik-Leibovich equation are equally valid, but might demand more changes in an existing numerical code. The energy transfer from the waves to the ocean can then be split-up into energy which goes into mean motions and energy which goes into sub-grid turbulence. The transfer to mean motions consists of the work done by the surface stress, i.e. $\overline{\mathbf{u}^L \cdot \overline{\boldsymbol{\tau}}_{oc}}$, and through temporal changes in the Stokes drift, $\int \overline{\mathbf{u}^L \cdot \partial_t \overline{\mathbf{u}}^S} dz$. The latter term is expected to be much weaker than the work done by the surface stress, but is able to force, for example, strong surface wave driven inertial oscillations. As the overall energy transfer from the surface waves model to the ocean Φ_{oc} can be estimated using Eq. (31), the remainder energy transfer is related to wave breaking, which goes directly into subgrid turbulence.

The wave models usually allow to incorporate the sea surface velocity to be included in the second term of Eq. 24, which accounts for wave refraction by horizontal shear in $\mathbf{u}^L|_{z=0}$. The surface velocity could be also used in the wave model to compute the relative wind $\mathbf{u}_{10}^{atm} - \mathbf{u}^L|_{z=0}$, with \mathbf{u}_{10}^{atm} being the atmospheric absolute wind at 10m. The relative wind rather than the absolute wind is often used in bulk formulations for the atmospheric stress τ_a . Note, however, that wave models seem very sensitive to the bulk formulation (see Couvelard et al. (2020) for a detailed discussion).

We here describe a rather simple method to utilize the Lagrangian velocity in ocean models. More sophisticated methods are suggested, for example using the generalized Lagrangian mean (Ardhuin et al. 2008) or vertically Lagrangian coordinates (Aiki and Greatbatch 2012). These phase-averaging methods follow the wave motions and allow for a concise treatment of the wavy surface. However, they are much more difficult to realize.

Acknowledgments. This paper is a contribution to the Collaborative Research Centre TRR 181 Energy Transfer in Atmosphere and Ocean funded by the Deutsche Forschungsgemeinschaft (DFG, German Research Foundation) Projektnummer 274762653.

Data availability statement. The numerical code, relevant model data, and scripts are available on Zenodo with the identifier <https://doi.org/10.5281/zenodo.10043904>.

References

- Aiki, H., and R. J. Greatbatch, 2012: Thickness-weighted mean theory for the effect of surface gravity waves on mean flows in the upper ocean. *J. Phys. Oceanogr.*, **42** (5), 725–747.
- Ali, A., K. H. Christensen, Ø. Breivik, M. Malila, R. P. Raj, L. B. an E. P. Chassignet, and M. Bakhoday-Paskyabi, 2019: A comparison of Langmuir turbulence parameterizations and key wave effects in a numerical model of the North Atlantic and Arctic Oceans. *Ocean Modelling*, **137**, 76–97.
- Ardhuin, F., and A. D. Jenkins, 2006: On the interaction of surface waves and upper ocean turbulence. *J. Phys. Oceanogr.*, **36** (3), 551–557.
- Ardhuin, F., N. Rasche, and K. A. Belibassakis, 2008: Explicit wave-averaged primitive equations using a generalized lagrangian mean. *Ocean Modelling*, **20** (1), 35–60.
- Ardhuin, F., and Coauthors, 2010: Semiempirical dissipation source functions for ocean waves. Part I: Definition, calibration, and validation. *J. Phys. Oceanogr.*, **40** (9), 1917–1941.
- Belcher, S. E., and Coauthors, 2012: A global perspective on Langmuir turbulence in the ocean surface boundary layer. *Geophys. Res. Lett.*, **39** (18).
- Breivik, Ø., K. Mogensén, J.-R. Bidlot, M. A. Balmaseda, and P. A. E. M. Janssen, 2015: Surface wave effects in the NEMO ocean model: Forced and coupled experiments. *J. Geophys. Res., Oceans*, **120** (4), 2973–2992.
- Broström, G., K. H. Christensen, M. Drivdal, and J. E. H. Weber, 2014: Note on Coriolis-Stokes force and energy. *Ocean Dynamics*, **64**, 1039–1045.
- Burchard, H., 2001: Simulating the wave-enhanced layer under breaking surface waves with two-equation turbulence models. *J. Phys. Oceanogr.*, **31** (11), 3133–3145.

- Chalikov, D., and M. Y. Belevich, 1993: One-dimensional theory of the wave boundary layer. *Boundary-Layer Meteorology*, **63**, 65–96.
- Couvelard, X., F. Lemarié, G. Samson, J.-L. Redelsperger, F. Ardhuin, R. Benshila, and G. Madec, 2020: Development of a two-way-coupled ocean–wave model: assessment on a global nemo (v3. 6)–ww3 (v6. 02) coupled configuration. *Geosci. Model Dev.*, **13** (7), 3067–3090.
- Craik, A. D. D., and S. Leibovich, 1976: A rational model for Langmuir circulations. *J. Fluid Mech.*, **73** (03), 401–426.
- Czeschel, L., and C. Eden, 2019: Internal wave radiation through surface mixed layer turbulence. *J. Phys. Oceanogr.*, **49** (7), 1827–1844.
- Ducros, F., P. Comte, and M. Lesieur, 1996: Large-eddy simulation of transition to turbulence in a boundary layer developing spatially over a flat plate. *J. Fluid Mech.*, **326**, 1–36.
- Eden, C., L. Czeschel, and D. Olbers, 2014: Toward energetically consistent ocean models. *J. Phys. Oceanogr.*, **44** (12), 3160–3184.
- Fan, Y., and S. M. Griffies, 2014: Impacts of parameterized Langmuir turbulence and nonbreaking wave mixing in global climate simulations. *J. Climate*, **27** (12), 4752–4775.
- Haney, S., B. Fox-Kemper, K. Julien, and A. Webb, 2015: Symmetric and geostrophic instabilities in the wave-forced ocean mixed layer. *J. Phys. Oceanogr.*, **45** (12), 3033–3056.
- Hanley, K. E., S. E. Belcher, and P. P. Sullivan, 2010: A global climatology of wind–wave interaction. *J. Phys. Oceanogr.*, **40** (6), 1263–1282.
- Harcourt, R. R., 2013: A second-moment closure model of Langmuir turbulence. *J. Phys. Oceanogr.*, **43** (4), 673–697.
- Harcourt, R. R., 2015: An improved second-moment closure model of Langmuir turbulence. *J. Phys. Oceanogr.*, **45** (1), 84–103.
- Hasselmann, K., 1970: Wave-driven inertial oscillations. *Geophys. and Astrophys. Fluid Dyn.*, **1** (3-4), 463–502.
- Holm, D. D., 1996: The ideal Craik-Leibovich equations. *Physica D: Nonlinear Phenomena*, **98** (2-4), 415–441.

- Huang, N. E., 1979: On surface drift currents in the ocean. *J. Fluid Mech.*, **91** (1), 191–208.
- Janssen, P. A., 2012: Ocean wave effects on the daily cycle in sst. *J. Geophys. Res., Oceans*, **117** (C11).
- Komen, G. J., L. Cavaleri, M. Donelan, K. Hasselmann, S. Hasselmann, and P. Janssen, 1996: *Dynamics and modelling of ocean waves*. Cambridge University Press.
- Leibovich, S., 1980: On wave-current interaction theories of Langmuir circulations. *J. Fluid Mech.*, **99** (4), 715–724.
- Li, Q., A. Webb, B. Fox-Kemper, A. Craig, G. Danabasoglu, W. G. Large, and M. Vertenstein, 2016: Langmuir mixing effects on global climate: WAVEWATCH III in CESM. *Ocean Modelling*, **103**, 145–160.
- Liu, B., K. Wu, and C. Guan, 2009: Wind energy input to the ekman-stokes layer: reply to comment by jeff a. polton. *Journal of Oceanography*, **65**, 669–673.
- McDougall, T. J., and P. C. McIntosh, 2001: The temporal-residual-mean velocity. part ii: Isopycnal interpretation and the tracer and momentum equations. *J. Phys. Oceanogr.*, **31** (5), 1222–1246.
- McIntyre, M., 1988: A note on the divergence effect and the Lagrangian-mean surface elevation in periodic water waves. *J. Fluid Mech.*, **189**, 235–242.
- McWilliams, J. C., E. Huckle, J. Liang, and P. P. Sullivan, 2014: Langmuir turbulence in swell. *J. Phys. Oceanogr.*, **44** (3), 870–890.
- McWilliams, J. C., P. P. Sullivan, and C.-H. Moeng, 1997: Langmuir turbulence in the ocean. *J. Fluid Mech.*, **334**, 1–30.
- Olbers, D., J. Willebrand, and C. Eden, 2012: *Ocean dynamics*. Springer Science & Business Media.
- Pollard, R. T., 1970: Surface waves with rotation: An exact solution. *J. Geophys. Res.*, **75** (30), 5895–5898.
- Polton, J. A., 2009: A wave averaged energy equation: Comment on “global estimates of wind energy input to subinertial motions in the Ekman-Stokes layer” by bin liu, kejian wu and changlong guan. *Journal of Oceanography*, **65**, 665–668.

- Polton, J. A., D. M. Lewis, and S. E. Belcher, 2005: The role of wave-induced coriolis–stokes forcing on the wind-driven mixed layer. *J. Phys. Oceanogr.*, **35** (4), 444–457.
- Sayol, J. M., A. Orfila, and L.-Y. Oey, 2016: Wind induced energy–momentum distribution along the Ekman–Stokes layer. application to the Western Mediterranean Sea climate. *Deep Sea Research Part I: Oceanographic Research Papers*, **111**, 34–49.
- Skyllingstad, E. D., and D. W. Denbo, 1995: An ocean large-eddy simulation of Langmuir circulations and convection in the surface mixed layer. *J. Geophys. Res.*, **100** (C5), 8501–8522.
- Stokes, G. G., 1847: On the theory of oscillatory waves. *Trans. Cam. Philos. Soc.*, **8**, 441–455.
- Sun, R. A., and Coauthors, 2022: Waves in SKRIPS: WaveWatch III coupling implementation and a case study of cyclone Mekunu. *EGUsphere*.
- Suzuki, N., and B. Fox-Kemper, 2016: Understanding Stokes forces in the wave-averaged equations. *J. Geophys. Res.*, **121** (5), 3579–3596.
- Teixeira, M. A. C., and S. E. Belcher, 2002: On the distortion of turbulence by a progressive surface wave. *J. Fluid Mech.*, **458**, 229–267.
- Ursell, F., and G. E. R. Deacon, 1950: On the theoretical form of ocean swell. On a rotating earth. *Geophysical Journal International*, **6**, 1–8.
- Vanneste, J., and W. R. Young, 2022: Stokes drift and its discontents. *Philos. Trans. Roy. Soc. London*, **380** (2225), 20210 032.
- Wagner, G. L., G. P. Chini, A. Ramadhan, B. Gallet, and R. Ferrari, 2021: Near-inertial waves and turbulence driven by the growth of swell. *J. Phys. Oceanogr.*, **51** (5), 1337–1351.
- WAVEWATCH III, R., 2016: Development group (WW3DG): User manual and system documentation of WAVEWATCH III R version 5.16. *Tech. Note 329, NOAA/NWS/NCEP/MMAB, College Park, MD, USA*.
- Weber, J. E. H., M. Drivdal, K. H. Christensen, and G. Broström, 2015: Some aspects of the Coriolis-Stokes forcing in the oceanic momentum and energy budgets. *Journal of Geophysical Research: Oceans*, **120** (8), 5589–5596.

Zhang, Y., Z. Song, K. Wu, and Y. Shi, 2019: Influences of random surface waves on the estimates of wind energy input to the Ekman layer in the Antarctic circumpolar current region. *Journal of Geophysical Research: Oceans*, **124** (5), 3393–3410.